arXiv:hep-ph/0001322v2 1 Feb 2000

Probe of CP Violation in $e^+e^- \to t\bar{t}$ Near Threshold

M. Jeżabek

Institute of Nuclear Physics, Kawiory 26a, PL-30055 Cracow, Poland
and
Department of Field Theory and Particle Physics, University of Silesia,
Uniwersytecka 4, PL-40007 Katowice, Poland

T. Nagano and Y. Sumino

Department of Physics, Tohoku University
Sendai, 980-8578 Japan

Abstract

We study how to probe the anomalous CP-violating couplings of top quark with γ, Z and g in the $t\bar{t}$ threshold region at future e^+e^- colliders. These couplings contribute to the difference of the t and $\bar{t}$ polarization vectors $\delta\mathbf{P}$ and to the CP-odd spin correlation tensor $\delta\mathbf{Q}_{ij}$. We find that typical sizes of $\delta\mathbf{P}$ and $\delta\mathbf{Q}_{ij}$ are 5–20% times the couplings $(d_{t\gamma}, d_{tZ}, d_{tg})$ in the threshold region. Experimentally $\delta\mathbf{P}$ can be measured efficiently using the CP-odd combination of the $\ell^\pm$ momenta or of the $\ell^\pm$ directions. We have similar sensitivities to both the real and imaginary parts of the couplings independently using the two components of $\delta\mathbf{P}$. Taking advantage of different dependences of $\delta\mathbf{P}$ on the $e^\pm$ polarizations and on the c.m. energy, we will be able to disentangle the effects of the three couplings $d_{t\gamma}$, d_{tZ}, d_{tg} in the $t\bar{t}$ threshold region. We give rough estimates of sensitivities to the anomalous couplings expected at future e^+e^- colliders. The sensitivities to $d_{t\gamma}$ and d_{tZ} are comparable to those attainable in the open-top region at e^+e^- colliders. The sensitivity to d_{tg} is worse than that expected at a hadron collider but exceeds the sensitivity in the open-top region at e^+e^- colliders.

1 Introduction

Among all the fermions included in the Standard Model (SM), the top quark plays a very unique role. The mass of top quark is by far the largest and approximates the electroweak symmetry breaking scale. In fact the top quark is the heaviest of all the elementary particles discovered up to now. It means that in the SM Lagrangian the top quark mass term breaks the $SU(2)_L \times U(1)_Y$ symmetry maximally. This fact suggests that the top quark couples strongly to the physics that breaks the electroweak symmetry. It is therefore important to investigate properties of top quark in detail, for the purpose of probing the symmetry breaking physics as well as to gain deeper understanding of the origin of the flavor structure. The standard procedures for investigating top quark properties are: measurements of fundamental quantities such as its mass and decay width; detailed examinations of various interactions of top quark to see if there are signs of new physics. Among them testing the CP-violating interactions of top quark is particularly interesting. This is because: (1) CP-violation in the top quark sector is extremely small within the SM. If any CP-violating effect is detected in the top sector in a near-future experiment, it immediately signals new physics. (2) There can be many sources of CP-violation in models that extend the SM, such as supersymmetric (SUSY) models, Leptoquark models (including R-parity violating SUSY models), multi-Higgs-doublet models, Extra-dimensions, etc. (3) In relatively wide class of models beyond the SM, CP-violation emerges especially sizably in the top quark sector.

Predictions of certain models are as follows. In the SM, the lowest-order contributions to the electric-dipole-moment (EDM) of a quark come from three loop diagrams and are proportional to $G_F^2 \alpha_s$ [1]. Assuming that the results for u- and d-quarks can also be applied to the top quark, one may estimate the top quark EDM as $\sim 10^{-30} e$ cm. One may also estimate the Z-EDM and chromo-EDM of top quark as $\sim 10^{-30} e$ cm and $\sim 10^{-30} g_s$ cm, respectively, since there seems to be no reason that these two EDMs are much suppressed or enhanced. All these EDMs of top quark are quite small compared to those corresponding to the "$\mathcal{O}(1)$-couplings", $e/m_t \sim 10^{-16} e$ cm and $g_s/m_t \sim 10^{-16} g_s$ cm. On the other hand, the top quark EDMs are induced at one loop in many models, including multi-Higgs-multiplet models and SUSY models. In the two-Higgs-doublet models, a neutral Higgs ϕ can violate CP through the Yukawa interaction $\bar{\psi}(a - \tilde{a}\gamma_5)\psi\,\phi$ [2–8]. The size of the induced EDM is estimated as* $\sim eG_F m_t^3/(4\pi^2 m_\phi^2) = 3 \times 10^{-18} e$ cm $(m_\phi/100\,\text{GeV})^{-2}$. The explicit calculations show somewhat smaller values, 10^{-18}–$10^{-20} e$ cm, depending on $\sqrt{s}$ and m_ϕ. In the Minimal SUSY Standard Model CP can be violated in the soft SUSY breaking sector [6, 8–11]. It was shown that the top quark EDM of $\sim 10^{-19} e$ cm can be induced by gluino and chargino exchanges, assuming a universal gaugino mass and non-universal other soft-breaking parameters.

Present experimental limits on the EDMs of top quark are not stringent [12]. A limit on the chromo-EDM $\lesssim 10^{-16} g_s$ cm is obtained from the analyses using $\sigma_{\text{tot}}(p\bar{p} \to t\bar{t}X)$ and p_T distributions of prompt photons produced in $qg \to q\gamma$, etc. at Tevatron and from the analyses using $\text{Br}(B \to X_s\gamma)$ at CLEO. The limit on the EDM from the prompt photon distribution is similar: EDM $\lesssim 10^{-16} e$ cm.

---

* Here, one power of m_t is necessary to flip chirality. The extra two powers of m_t come from the Yukawa interaction.

There have been a number of sensitivity studies on the top quark EDMs expected at future hadron colliders and in the open-top region ($\sqrt{s} \gg 2m_t$) at future e^+e^- and $\gamma\gamma$ colliders. In hadron collider studies [3, 4, 10, 13–16], it is claimed that with the observables[†] made of elaborated combinations of momenta of charged leptons, b-quarks, etc., experiments at $\sqrt{s} = 500\,\mathrm{GeV}$ and with an integrated luminosity $10\,\mathrm{fb}^{-1}$ can probe the chromo-EDM down to a few $\times 10^{-17}$–$10^{-18} g_s$ cm, or even to a few $\times 10^{-19} g_s$ cm by raising complexity of the observables. However, none of them performs detector simulations, which seem to be indispensable for a serious sensitivity study.[‡] Among several proposed CP-odd observables, lepton energy asymmetry $A_E^\ell = E_{\ell^+} - E_{\ell^-}$ would be the simplest one [3, 10, 15]. It is claimed that A_E^ℓ is sensitive to the imaginary part[§] of the chromo-EDM down to $\sim 10^{-18} g_s$ cm assuming an acceptance efficiency $\epsilon = 10\%$. Also studies of the EDM and Z-EDM of top quark in the open-top region at e^+e^- colliders are given in [5–8, 11, 16–20]. We take as a reference the results of [17], which is based on simulation studies incorporating experimental conditions expected at a future e^+e^- linear collider. It is shown that, by using the mode $t\bar{t} \to b\bar{b}WW \to b\bar{b}q\bar{q}'\ell\nu$ ($\ell = e, \mu$), sensitivities to (the real and imaginary parts of) the EDM and Z-EDM are $\sim 10^{-17} e$ cm at $\sqrt{s} = 500\,\mathrm{GeV}$, assuming an integrated luminosity of $10\,\mathrm{fb}^{-1}$ and electron beam polarization of $\pm 80\%$. Sensitivity to the top chromo-EDM in the open-top region at e^+e^- colliders is studied in [21]; they estimate a sensitivity $\sim 10^{-16} g_s$ cm at $\sqrt{s} = 500\,\mathrm{GeV}$, assuming an integrated luminosity $50\,\mathrm{fb}^{-1}$, an identification efficiency for top-pair production events $\simeq 100\%$, and $E_g^{\min} = 25\,\mathrm{GeV}$. The last entry is a cut for the minimum gluon-jet energy, on which the sensitivity depends crucially. No detector simulation is performed in this study. The sensitivities of $\gamma\gamma$ colliders are studied in [7, 8, 22]; they are shown to be similar to those of e^+e^- colliders.

Certainly it is desirable to probe the top quark anomalous interactions at highest possible energy where we have more resolving power, which motivated the above studies. On the other hand, it is known that studying various top quark properties in the $t\bar{t}$ threshold region at future e^+e^- colliders is promising and interesting; particularly the top quark mass will be determined to unmatched precision. A number of analyses elucidated physics potential of experiments in the $t\bar{t}$ threshold region [23–35]. Most of them, however, dealt only with the SM interactions. In this paper we extend these analyses and study how to probe anomalous CP-violating interactions of top quark in the $t\bar{t}$ threshold region. We note that there are some specific advantages in this region:

- The polarization of top quark can be raised to close to 100% by adjusting longitudinal polarization of e^- beam [36, 30].

- Since top quarks are produced almost at rest, one can reconstruct the spin information of top quarks from distributions of their decay products without solving detailed kinematics [31].

- The QCD interaction is enhanced in this region, so the cross section is sensitive to the

---

[†] They include the so-called "optimal observables" [13, 18].

[‡] For instance, it is important to study the effects of mis-assignment of jets to partons in event reconstructions.

[§] Note that A_E^ℓ probes absorptive part of an amplitude $\mathcal{M}$, since it is $C\tilde{P}T$-odd.

top-gluon (tg) couplings. We can study anomalous tg couplings in a clean environment in comparison to hadron colliders.

- There are less backgrounds from multiple W,Z productions compared to the open-top region.

- In certain models (e.g. those in which a neutral Higgs is exchanged between t and $\bar{t}$ [2]), the induced top quark EDM and Z-EDM are enhanced near the $t\bar{t}$ threshold.

Thus, for the sake of comparison with other kinematical regions, we would like to know sensitivities to CP-violation achievable in $e^+e^- \to t\bar{t}$ in the threshold region when these advantages are taken into account.

In Sec. 2 we present a qualitative picture of the effects of the anomalous CP-violating interactions in the threshold region. We derive the top quark vertices including the QCD enhancement in Sec. 3. The formulas for the polarization vectors and the spin correlation tensor of t and $\bar{t}$ are presented in Sec. 4, followed by their numerical analyses in Sec. 5. Sec. 6 discusses the observables to be measured in experiments and gives rough estimates of sensitivities to the anomalous couplings. We summarize and conclude our analyses in Sec. 7. Some of the notations used in this paper are collected in the Appendix.

2   Physical Picture

Let us first review the time evolution of t and $\bar{t}$, pair-created in e^+e^- collision just below threshold, within the SM. They are created close to each other at a relative distance $r \sim 1/m_t$ and then spread apart non-relativistically. When their relative distance becomes of the order of the Bohr radius, $r \sim (\alpha_s m_t)^{-1}$, they start to form a Coulombic boundstate. When the relative distance becomes $r \sim (m_t \Gamma_t)^{-1/2}$, where Γ_t is the decay width of top quark, either t or $\bar{t}$ decays via electroweak interaction, and accordingly the boundstate decays. Numerically these two scales have similar magnitudes, $(\alpha_s m_t)^{-1} \sim (m_t \Gamma_t)^{-1/2}$, and are much smaller than the hadronization scale $\sim 1/\Lambda_{\mathrm{QCD}}$. Since gluons which have wavelengths much longer than the size of the $t\bar{t}$ system cannot couple to this color singlet system, the strong interaction participating in the formation of the boundstate is dictated by the perturbative domain of QCD. The spin and PC of the dominantly produced boundstate are $J^{PC} = 1^{--}$. Inside this boundstate: t and $\bar{t}$ are in the S-wave state ($L = 0$); the spins of t and $\bar{t}$ are aligned to each other and pointing to e^- beam direction $|\uparrow\uparrow\rangle$ or to e^+ beam direction $|\downarrow\downarrow\rangle$ or they are in a linear combination of the two states ($S = 1$).

In this paper we consider anomalous CP-violating interactions of top quark with γ, Z, and g. In particular, we consider the lowest dimension effective operators which violate CP:

$$\mathcal{L}_{CP\text{-odd}} = -\frac{ed_{t\gamma}}{2m_t}(\bar{t}i\sigma^{\mu\nu}\gamma_5 t)\partial_\mu A_\nu - \frac{g_Z d_{tZ}}{2m_t}(\bar{t}i\sigma^{\mu\nu}\gamma_5 t)\partial_\mu Z_\nu - \frac{g_s d_{tg}}{2m_t}(\bar{t}i\sigma^{\mu\nu}\gamma_5 T^a t)\partial_\mu G_\nu^a \;,$$

$$\sigma^{\mu\nu} \equiv \tfrac{i}{2}[\gamma^\mu, \gamma^\nu] \;, \qquad (1)$$

where $e = g_W \sin\theta_W$ and $g_Z = g_W/\cos\theta_W$. These represent the interactions of γ, Z, g with

Figure 1: The diagrams which contribute to the spin-dependent CP-violating potential between non-relativistic t and $\bar{t}$. The vertex $\otimes$ represents the CP-odd interaction of top quark with gluon; cf. eq. (1). An exchange of the Coulomb gluon g^{C} gives the leading contribution of the CP-odd interaction to the potential.

the EDM, Z-EDM, chromo-EDM of top quark, respectively.[¶] Each of these interactions has $C = +1$ and $P = -1$. We assume that generally the anomalous couplings $d_{t\gamma}$, d_{tZ}, d_{tg} are complex where their imaginary parts may be induced from some absorptive processes beyond the SM. For a non-relativistic $t\bar{t}$ pair produced in $e^{+}e^{-}$ collision, the anomalous couplings of $t\bar{t}$ to γ and Z reduce to

$$\frac{ed_{t\gamma}}{m_t} \boldsymbol{A} \cdot \chi_{\bar{t}}^{\dagger}(-i\nabla)\chi_t + \frac{g_Z d_{tZ}}{m_t} \boldsymbol{Z} \cdot \chi_{\bar{t}}^{\dagger}(-i\nabla)\chi_t, \tag{2}$$

where χ_t and $\chi_{\bar{t}}$ denote the two-component non-relativistic fields of t and $\bar{t}$, respectively. The anomalous top-gluon coupling generates effectively a spin-dependent potential between t and $\bar{t}$

$$V_{CP\text{-odd}} = \frac{d_{tg}}{m_t} \left(\boldsymbol{s}_t - \bar{\boldsymbol{s}}_t \right) \cdot \nabla V_{\mathrm{C}}(r) \tag{3}$$

through the diagrams shown in Fig. 1. Here, $\boldsymbol{s}_t$ and $\bar{\boldsymbol{s}}_t$ denote the spins of non-relativistic t and $\bar{t}$, respectively; $V_{\mathrm{C}}(r) = -C_F \alpha_s/r$ is the Coulomb potential with the color factor $C_F = 4/3$. When $d_{tg} > 0$, the potential $V_{CP\text{-odd}}$ tends to align both chromo-EDMs in the direction of chromo-electric field, or, align $\bar{\boldsymbol{s}}_t$ in the direction of $\boldsymbol{r} = \boldsymbol{r}_t - \bar{\boldsymbol{r}}_t$ and $\boldsymbol{s}_t$ in the direction of $-\boldsymbol{r}$.

Let us consider effects of these anomalous interactions on the time evolution of the $t\bar{t}$ system. Assuming that the anomalous couplings $d_{t\gamma}$, d_{tZ}, d_{tg} are small, we consider the effects which arise in linear perturbation in these couplings. CP-violation originating from the $t\gamma$ or tZ coupling occurs at the stage of the pair creation, i.e. when t and $\bar{t}$ are very close to each other. The generated boundstate has $J^{PC} = 1^{+-}$, so t and $\bar{t}$ are in the P-wave ($L = 1$) and spin-0 state $|\uparrow\downarrow\rangle - |\downarrow\uparrow\rangle$. On the other hand, CP-violation originating from the tg coupling takes place after the boundstate formation when multiple gluons are exchanged between t and $\bar{t}$, i.e. when t and $\bar{t}$ are separated at a distance of the Bohr radius. Therefore, first the boundstate is formed in $J^{PC} = 1^{--}$ ($L = 0$ and $S = 1$) state and after interacting via the potential $V_{CP\text{-odd}}$ it turns into $J^{PC} = 1^{+-}$ ($L = 1$ and $S = 0$) state. Since we are interested in the dependences of observables on the couplings $d_{t\gamma}$, d_{tZ}, d_{tg} up to linear terms, we are interested in the interference of the leading SM amplitude and the amplitude including these couplings. The strong phases of these amplitudes that arise from QCD binding effects can be calculated reliably using perturbative QCD.

[¶] The magnitudes of these EDMs are given by $ed_{t\gamma}/m_t$, $g_Z d_{tZ}/m_t$, $g_s d_{tg}/m_t$, respectively.

Which CP-odd observables are sensitive to the above CP-violating couplings? For the process $e^+e^- \to t\bar{t}$, we may conceive of following expectation values of combinations of kinematical variables for CP-odd observables:

$$\langle\, (\boldsymbol{p}_e - \bar{\boldsymbol{p}}_e)\cdot(\boldsymbol{s}_t - \bar{\boldsymbol{s}}_t)\,\rangle,$$
$$\langle\, (\boldsymbol{p}_t - \bar{\boldsymbol{p}}_t)\cdot(\boldsymbol{s}_t - \bar{\boldsymbol{s}}_t)\,\rangle, \tag{4}$$
$$\langle\, [(\boldsymbol{p}_e - \bar{\boldsymbol{p}}_e)\times(\boldsymbol{p}_t - \bar{\boldsymbol{p}}_t)]\cdot(\boldsymbol{s}_t - \bar{\boldsymbol{s}}_t)\,\rangle,$$

where the spins and momenta are defined in the c.m. frame. (The initial state is CP-even if we assume the SM interactions of $e^\pm$ with γ and Z.) Generally one may think of other combinations involving $\boldsymbol{s}_e$ and $\bar{\boldsymbol{s}}_e$ as well. However, the spin directions of $e^\pm$ are not independent of their momentum directions for longitudinally polarized or unpolarized beams. Therefore, we would like to measure the difference of the spins (or the polarization vectors) of t and $\bar{t}$. Practically we can measure the t and $\bar{t}$ polarization vectors efficiently using $\ell^\pm$ angular distributions. It is known that the angular distribution of the charged lepton ℓ^+ from the decay of top quark is maximally sensitive to the top quark polarization vector. In the rest frame of top quark, the ℓ^+ angular distribution is given by [37]

$$\frac{1}{\Gamma_t}\frac{d\Gamma(t\to b\ell^+\nu)}{d\cos\theta_{\ell^+}} = \frac{1 + P\cos\theta_{\ell^+}}{2} \tag{5}$$

at tree level, where P is the top quark polarization and θ_{ℓ^+} is the angle of ℓ^+ measured from the direction of the top quark polarization vector.[||] Furthermore, we may think of CP-odd observables bilinear in $\boldsymbol{s}_t$ and $\bar{\boldsymbol{s}}_t$, which require more complicated analyses for their reconstructions from decay products.

We may anticipate following aspects of the CP-odd quantity $\delta\mathbf{P} = (\mathbf{P} - \bar{\mathbf{P}})/2$, (a half of) the difference of the t and $\bar{t}$ polarization vectors. It will be directly proportional to the coupling $d_{t\gamma}$ or d_{tZ} or d_{tg} when only one of the couplings is turned on at a time. $\delta\mathbf{P}$ will include a suppression factor $\beta \simeq |\boldsymbol{p}_t|/m_t$, the top quark velocity, since these couplings are accompanied by the top quark momentum; cf. eqs. (2) and (3). Thus, this factor will be larger at higher c.m. energy. Apart from this β, energy dependence of $\delta\mathbf{P}$ originating from the anomalous tg coupling will be different from that originating from the anomalous $t\gamma$ and tZ couplings. The contribution of the coupling d_{tg} to $\delta\mathbf{P}$ will be suppressed if the energies of t and $\bar{t}$ are too large to allow for enhancement of QCD due to Coulomb binding effects. This happens if the c.m. energy measured from the threshold $\mathcal{E} = \sqrt{s} - 2m_t$ is much larger than the Coulomb binding energy, $\mathcal{E} \gg \alpha_s^2 m_t$. On the other hand, the contribution of $d_{t\gamma}$ or d_{tZ} coupling would not have such energy dependence since CP violation occurs at the first stage of the top pair production. Dependences of $\delta\mathbf{P}$ on the e^- longitudinal polarization will be different between the photon-induced effect and the Z-induced effect, since e_L and e_R couple differently to γ and Z. These differences in the energy and e^- polarization dependences can be used to disentangle the effects of the three anomalous CP violating interactions in the $t\bar{t}$ threshold region.[**]

[||] Indeed the ℓ^+ distribution is ideal for extracting CP-violation in the $t\bar{t}$ production process; the above angular distribution is unchanged even if anomalous interactions are included in the tbW decay vertex, up to the terms linear in the decay anomalous couplings and within the approximation $m_b = 0$ [38].

[**] Use of the e^- longitudinal polarization for decomposing the photon-induced effect and the Z-induced effect was advocated in [20].

6

3 The Top Production Vertices

In this section we present the $t\bar{t}\gamma$ and $t\bar{t}Z$ vertices when the QCD binding effects and the CP-violating anomalous couplings are included. At tree level (and without anomalous interactions), the electroweak $t\bar{t}$ vertices are given by

$$\left(\Gamma^X\right)^i = v^{tX}\Gamma_V^i - a^{tX}\Gamma_A^i \ , \qquad \Gamma_V^i = \gamma^i \ , \quad \Gamma_A^i = \gamma^i\gamma_5 \qquad (X = \gamma, Z) \ , \qquad (6)$$

times $-ig_X$. Since the vertex $(\Gamma^X)^\mu$ is contracted with the wave functions of γ and Z produced by e^+e^- annihilation, only the space components of $(\Gamma^X)^\mu$ are relevant. Here and hereafter, the Latin indices refer to the space components. See Appendix for the definition of the electroweak couplings g_X, v^{tX} and a^{tX}. These vertices are modified by the QCD binding effects and by the anomalous interactions as

$$\left(\Gamma^X\right)^i = v^{tX}\Gamma_V^i - a^{tX}\Gamma_A^i + d_{tX}\Gamma_{X\text{-EDM}}^i \ , \qquad (7)$$

where

$$\Gamma_V^i = \left[\left(1 - \frac{2C_F\alpha_s}{\pi}\right)\gamma^i G(E,p) + i\gamma_5\frac{p^i}{m_t}d_{tg}D(E,p)\right] \times \left(\frac{\boldsymbol{p}^2}{m_t} - (E + i\Gamma_t)\right) \ ,$$

$$\Gamma_A^i = \left(1 - \frac{C_F\alpha_s}{\pi}\right)\gamma^i\gamma_5 F(E,p) \times \left(\frac{\boldsymbol{p}^2}{m_t} - (E + i\Gamma_t)\right) \ , \qquad (8)$$

$$\Gamma_{X\text{-EDM}}^i = -i\gamma_5\frac{p^i}{m_t}F(E,p) \times \left(\frac{\boldsymbol{p}^2}{m_t} - (E + i\Gamma_t)\right) \ .$$

$\boldsymbol{p} = \boldsymbol{p}_t = -\bar{\boldsymbol{p}}_t$ denotes the top quark momentum in the c.m. frame, and $p = |\boldsymbol{p}|$. We work in the potential-subtracted-mass scheme [39] instead of the pole-mass scheme, and $E = \sqrt{s} - 2m_{\text{PS}}(\mu_f)$ represents the c.m. energy measured from the twice of the potential-subtracted mass of top quark; m_t denotes the pole mass of top quark and it is expressed in terms of the potential-subtracted mass by

$$m_t = m_{\text{PS}}(\mu_f) + \frac{C_F\alpha_s(\mu)}{\pi}\mu_f\left[1 + \frac{\alpha_s(\mu)}{4\pi}\left\{a_1 - \beta_0\left(\log\frac{\mu_f^2}{\mu^2} - 2\right)\right\}\right] \qquad (9)$$

with

$$a_1 = \frac{31}{9}C_A - \frac{20}{9}T_F n_f \ , \quad \beta_0 = \frac{11}{3}C_A - \frac{4}{3}T_F n_f \ , \qquad (10)$$

where μ_f and μ denote the renormalization scale of the potential-subtracted mass and the $\overline{\text{MS}}$ coupling, respectively; $C_F = 4/3$, $C_A = 3$, $T_F = 1/2$ are the color factors and $n_f = 5$ is the number of active flavors.

$G(E,p)$ and $F(E,p)$ are the S-wave and P-wave Green functions, respectively, defined by

$$\left[-\frac{\nabla^2}{m_t} + V(r;\mu_f) - (E + i\Gamma_t)\right]\tilde{G}(E,\boldsymbol{x}) = \delta^3(\boldsymbol{x}) \ , \qquad (11)$$

$$\left[-\frac{\nabla^2}{m_t} + V(r;\mu_f) - (E + i\Gamma_t)\right]\tilde{F}^k(E,\boldsymbol{x}) = -i\partial^k\delta^3(\boldsymbol{x}) \ , \qquad (12)$$

and

$$G(E,p) \;=\; \int d^3\boldsymbol{x}\, e^{-i\boldsymbol{p}\cdot\boldsymbol{x}}\, \tilde{G}(E,\boldsymbol{x})\;, \tag{13}$$

$$p^k\, F(E,p) \;=\; \int d^3\boldsymbol{x}\, e^{-i\boldsymbol{p}\cdot\boldsymbol{x}}\, \tilde{F}^k(E,\boldsymbol{x})\;. \tag{14}$$

$V(r;\mu_f)$ is the Fourier transform of the two-loop renormalization-group-improved QCD potential, where the infrared renormalon-pole is subtracted and absorbed into the definition of $m_{\rm PS}(\mu_f)$. See [34] for details. One may also write conveniently as

$$G(E,p) = \langle\boldsymbol{p}| \frac{1}{\boldsymbol{p}^2/m_t + V - (E + i\Gamma_t)} |\boldsymbol{x} = \vec{0}\rangle\;, \tag{15}$$

$$\boldsymbol{p}F(E,p) = \langle\boldsymbol{p}| \frac{1}{\boldsymbol{p}^2/m_t + V - (E + i\Gamma_t)} \boldsymbol{p}|\boldsymbol{x} = \vec{0}\rangle\;. \tag{16}$$

The Green function associated with the gluon anomalous coupling is given by

$$D(E,p) = G(E,p) - F(E,p). \tag{17}$$

We can see from eqs. (8) that the effects of all the anomalous CP-violating interactions are suppressed by $|\boldsymbol{p}|/m_t \simeq \beta$. Thus, for consistency we have incorporated all $\mathcal{O}(\alpha_s) = \mathcal{O}(\beta)$ corrections in the SM vertices.

A sketch of derivations of these vertices goes as follows. Using non-relativistic forms of the t and $\bar{t}$ propagators,

$$S_F(k^\mu + \frac{q^\mu}{2}) \simeq \frac{1 + \gamma^0}{2} \frac{i}{\mathcal{E}/2 + k^0 - |\boldsymbol{k}|^2/(2m_t) + i\Gamma_t/2}\;,$$
$$S_F(k^\mu - \frac{q^\mu}{2}) \simeq \frac{1 - \gamma^0}{2} \frac{i}{\mathcal{E}/2 - k^0 - |\boldsymbol{k}|^2/(2m_t) + i\Gamma_t/2}\;, \tag{18}$$

where $q^\mu = (2m_t + \mathcal{E}, \vec{0})$ and $k^\mu = (k^0, \boldsymbol{k})$ in the c.m. frame, a self-consistent equation for the vector vertex, similar to that given in [24], reads

$$\Gamma^i_V(\mathcal{E}, p^\mu) = \gamma^i + C_F(-ig_s)^2 \int \frac{{\rm d}^4 k}{(2\pi)^4} \frac{i}{\mathcal{E}/2 + k^0 - |\boldsymbol{k}|^2/(2m_t) + i\Gamma_t/2} \times$$
$$\times \frac{i}{\mathcal{E}/2 - k^0 - |\boldsymbol{k}|^2/(2m_t) + i\Gamma_t/2} \times$$
$$\times \Bigg[\quad \gamma^0 \frac{1 + \gamma^0}{2} \Gamma^i_V(\mathcal{E}, k^\mu) \frac{1 - \gamma^0}{2} \gamma^0$$
$$- \left(\frac{d_{tg}}{2m_t}\right) \sigma^{j0} \gamma_5 (p - k)^j \frac{1 + \gamma^0}{2} \Gamma^i_V(\mathcal{E}, k) \frac{1 - \gamma^0}{2} \gamma^0$$
$$+ \left(\frac{d_{tg}}{2m_t}\right) \gamma^0 \frac{1 + \gamma^0}{2} \Gamma^i_V(\mathcal{E}, k) \frac{1 - \gamma^0}{2} \sigma^{j0} \gamma_5 (p - k)^j$$
$$\Bigg] \times \frac{i}{|\boldsymbol{p} - \boldsymbol{k}|^2}\;. \tag{19}$$

Since there is no p^0-dependence on the right-hand-side, consistency requires $\Gamma_V^i(\mathcal{E}, p^\mu) = \Gamma_V^i(\mathcal{E}, \boldsymbol{p})$. Thus we can trivially integrate over p^0 and obtain

$$
\Gamma_V^i(\mathcal{E}, \boldsymbol{p}) = \gamma^i - \int \frac{\mathrm{d}^3 \boldsymbol{k}}{(2\pi)^3} \frac{-C_F g_s^2}{|\boldsymbol{p} - \boldsymbol{k}|^2} \frac{1}{|\boldsymbol{k}|^2/m_t - (\mathcal{E} + i\Gamma_t)} \times
$$
$$
\times \frac{1 + \gamma^0}{2} \left[\Gamma_V^i(\mathcal{E}, \boldsymbol{k}) - \frac{d_{tg}}{2m_t}(p - k)^j \left\{ \sigma^{j0} \gamma_5 \Gamma_V^i(\mathcal{E}, \boldsymbol{k}) + \Gamma_V^i(\mathcal{E}, \boldsymbol{k}) \sigma^{j0} \gamma_5 \right\} \right] \frac{1 - \gamma^0}{2} .
$$
$$(20)$$

We decompose the vertex function $\Gamma_V^i(\mathcal{E}, \boldsymbol{p})$ into different spinor structures as

$$
\frac{1 + \gamma^0}{2} \Gamma_V^i(\mathcal{E}, \boldsymbol{p}) \frac{1 - \gamma^0}{2} = \frac{1 + \gamma^0}{2} \left[\gamma^i \Gamma_G(\mathcal{E}, p) + \gamma^j \left(\frac{p^i p^j}{|\boldsymbol{p}|^2} - \frac{1}{3} \delta^{ij} \right) \Gamma_B(\mathcal{E}, p) \right.
$$
$$
\left. + \gamma^i \gamma_5 \Gamma_F(\mathcal{E}, p) + i\gamma_5 \frac{p^i}{m_t} \Gamma_D(\mathcal{E}, p) \right] \frac{1 - \gamma^0}{2}.
$$
$$(21)$$

By pluging this expression into the integral equation above, one obtains integral equations for scalar functions $\Gamma_G(\mathcal{E}, p)$, etc. One can see that $\Gamma_D(\mathcal{E}, p) = \mathcal{O}(d_{tg})$, $\Gamma_B(\mathcal{E}, p) = \mathcal{O}(d_{tg}^2)$. Thus we neglect $\Gamma_B(\mathcal{E}, p)$ hereafter. Let us write

$$
\Gamma_G(\mathcal{E}, p) = \left(\frac{\boldsymbol{p}^2}{m_t} - (\mathcal{E} + i\Gamma_t) \right) G(\mathcal{E}, p) ,
$$
$$
\Gamma_F(\mathcal{E}, p) = \left(\frac{\boldsymbol{p}^2}{m_t} - (\mathcal{E} + i\Gamma_t) \right) F(\mathcal{E}, p) ,
$$
$$(22)$$
$$
\Gamma_D(\mathcal{E}, p) = \left(\frac{\boldsymbol{p}^2}{m_t} - (\mathcal{E} + i\Gamma_t) \right) d_{tg} D(\mathcal{E}, p) .
$$

Then G, F and D satisfy

$$
\left(\frac{\boldsymbol{p}^2}{m_t} - (\mathcal{E} + i\Gamma_t) \right) G(\mathcal{E}, p) + \int \frac{\mathrm{d}^3 \boldsymbol{k}}{(2\pi)^3} \widetilde{V}_{\mathrm{C}}(|\boldsymbol{p} - \boldsymbol{k}|) G(\mathcal{E}, k) = 1 , \tag{23}
$$

$$
\left(\frac{\boldsymbol{p}^2}{m_t} - (\mathcal{E} + i\Gamma_t) \right) p^i F(\mathcal{E}, p) + \int \frac{\mathrm{d}^3 \boldsymbol{k}}{(2\pi)^3} \widetilde{V}_{\mathrm{C}}(|\boldsymbol{p} - \boldsymbol{k}|) k^i F(\mathcal{E}, k) = p^i , \tag{24}
$$

$$
\left(\frac{\boldsymbol{p}^2}{m_t} - (\mathcal{E} + i\Gamma_t) \right) p^i D(\mathcal{E}, p) + \int \frac{\mathrm{d}^3 \boldsymbol{k}}{(2\pi)^3} \widetilde{V}_{\mathrm{C}}(|\boldsymbol{p} - \boldsymbol{k}|) k^i D(\mathcal{E}, k)
$$
$$
= \int \frac{\mathrm{d}^3 \boldsymbol{k}}{(2\pi)^3} \widetilde{V}_{\mathrm{C}}(|\boldsymbol{p} - \boldsymbol{k}|)(k - p)^i G(\mathcal{E}, k) \tag{25}
$$

with $\widetilde{V}_{\mathrm{C}}(q) = -C_F 4\pi \alpha_s/q^2$. Comparing the third equation with the first two equations, we find that $D = G - F$. The first two equations are equivalent to eqs. (11)-(16) apart from the fact that the Coulomb potential $-C_F \alpha_s/r$ is replaced by* $V(r; \mu_f)$ and that the renormalization-group-improved potential-subtracted-mass scheme [34] is used instead of the pole-mass scheme.

---

* The replacement is justified: In Coulomb gauge the $\mathcal{O}(\alpha_s)$ corrections to the potential come solely from the vacuum polarization of Coulomb-gluon [40]. Hence, the net effect is to replace the fixed-coupling constant $\alpha_s(\mu)$ in the leading-order by the V-scheme running coupling constant $\alpha_V(|\boldsymbol{p} - \boldsymbol{k}|)$.

The axial-vector vertex was derived in [27]:

$$\Gamma_A^i \simeq \left(\frac{p^2}{m_t} - (E + i\Gamma_t) \right) \gamma^i \gamma_5 F(E, p) \ . \tag{26}$$

The hard-vertex factor for the vector vertex was derived in [41] and that for the axial-vector vertex in [42]. We may also derive $\Gamma_{X\text{-EDM}}^i$ in a similar manner.

Two comments would be in order here. One might think that including the non-renormalizable interactions eq. (1) into loop integrals [e.g. eq. (19)] causes ultra-violet divergences and leads to unpredictability. We note that only non-relativistic domains of the loop integrals are relevant in resummations of the Coulomb singularities. In fact high momentum regions are effectively cut off in the self-consistent equations due to our non-relativistic approximation. Thus, we can calculate unambiguously the leading contributions of these effective interactions. In this regard, in eqs. (8) the hard-vertex correction factors are associated only with the SM contributions. We cannot determine hard-vertex corrections to the vertices including the anomalous interactions since non-renormalizability of these interactions matters at this order.

The simple form of the Green function including the tg anomalous interaction eq. (17) is a consequence of the following fact. The effect of $V_{CP\text{-odd}}$ integrated over the time interval from $t = 0$ to $t = T$ can be written as $(d_{tg}/m_t) \left(\boldsymbol{s}_t - \bar{\boldsymbol{s}}_t \right) \cdot [\boldsymbol{p}(0) - \boldsymbol{p}(T)]$ using the equation of motion $\dot{\boldsymbol{p}} = -\nabla V_{\mathrm{C}}$. Namely the difference of the top quark momenta at $t = 0$ and at $t = T$ carries the net effect of the chromo-electric field which aligns the EDMs during $0 < t < T$. Concisely, for $H = \boldsymbol{p}^2/m_t + V_{\mathrm{C}}$ and $\delta H = V_{CP\text{-odd}}$, the variation of the time evolution of the $t\bar{t}$ system is expressed as

$$\delta \left(e^{-iHT} \right) = i \left[\frac{d_{tg}}{m_t} \left(\boldsymbol{s}_t - \bar{\boldsymbol{s}}_t \right) \cdot \boldsymbol{p} \ , \ e^{-iHT} \right] \ . \tag{27}$$

Thus, the propagation at a fixed energy is given by $(id_{tg}/m_t) \left(\boldsymbol{s}_t - \bar{\boldsymbol{s}}_t \right) \cdot \boldsymbol{p}(G - F)$; cf. eqs. (15) and (16).

4   The Polarization Vectors and the Spin Correlation Tensor of t and $\bar{t}$

Using the vertices derived in the previous section we may write down the production cross section of a $t\bar{t}$ pair in the threshold region. The cross section, where $(t, \bar{t})$ have momenta $(\boldsymbol{p}_t, -\boldsymbol{p}_t)$ and the spins $+\frac{1}{2}$ along the quantization axes $(\boldsymbol{s}_t, \bar{\boldsymbol{s}}_t)$ in the c.m. frame, is given by

$$\frac{\mathrm{d}\sigma(\boldsymbol{s}_t, \bar{\boldsymbol{s}}_t)}{\mathrm{d}^3\boldsymbol{p}_t} = \frac{\mathrm{d}\sigma}{\mathrm{d}^3\boldsymbol{p}_t} \frac{1 + \mathbf{P}\cdot\boldsymbol{s}_t + \bar{\mathbf{P}}\cdot\bar{\boldsymbol{s}}_t + (\boldsymbol{s}_t)_i (\bar{\boldsymbol{s}}_t)_j \mathbf{Q}_{ij}}{4} \ . \tag{28}$$

Here, $|\boldsymbol{s}_t| = |\bar{\boldsymbol{s}}_t| = 1$. On the right-hand-side, $\mathrm{d}\sigma/\mathrm{d}^3\boldsymbol{p}_t$ represents the production cross section when the spins of t and $\bar{t}$ are summed over:

$$\frac{\mathrm{d}\sigma}{\mathrm{d}^3\boldsymbol{p}_t} = \left(1 - \frac{4C_F \alpha_s}{\pi} \right) \frac{N_C \alpha^2 \Gamma_t}{2\pi m_t^4} \frac{1 - \mathrm{P}_{e^+}\mathrm{P}_{e^-}}{2}$$

$$\times |G(E, p_t)|^2 (a_1 + \chi a_2) \left\{ 1 + 2\mathrm{Re} \left[C_{\mathrm{FB}} \frac{F(E, p_t)}{G(E, p_t)} \right] \beta \cos\theta_{te} \right\} \ , \tag{29}$$

where $\beta = |\boldsymbol{p}_t|/m_t$ and $\cos\theta_{te} = \boldsymbol{p}_e \cdot \boldsymbol{p}_t/(|\boldsymbol{p}_e| \, |\boldsymbol{p}_t|)$; α is the fine structure constant; $N_c = 3$ is the number of colors; χ is a function of the initial $e^\pm$ longitudinal polarizations $P_{e\pm}$:

$$\chi = \frac{P_{e^+} - P_{e^-}}{1 - P_{e^+}P_{e^-}} \ . \tag{30}$$

If the positron beam is unpolarized ($P_{e^+} = 0$), $\chi = -P_{e^-}$. The coefficient C_{FB} and the constants a_1, a_2 are defined below.

In eq. (28) $\mathbf{P}$ and $\bar{\mathbf{P}}$ represent the polarization vectors of t and $\bar{t}$, respectively. Both the SM and the anomalous interactions contribute to the polarizations:

$$\mathbf{P} = \mathbf{P}_{\mathrm{SM}} + \delta\mathbf{P} \ , \quad \bar{\mathbf{P}} = \bar{\mathbf{P}}_{\mathrm{SM}} + \delta\bar{\mathbf{P}} \ . \tag{31}$$

The SM contributions are CP-even (except for tiny CP-violating effects which we neglect) and are equal for t and $\bar{t}$. On the other hand, the anomalous CP-odd contributions are opposite in sign:

$$\bar{\mathbf{P}}_{\mathrm{SM}} = \mathbf{P}_{\mathrm{SM}} \ , \quad \delta\bar{\mathbf{P}} = -\delta\mathbf{P} \ . \tag{32}$$

Note that we are working up to linear terms in the anomalous couplings. Hereafter we express these vectors by components:

$$\mathbf{P} = \mathrm{P}_{/\!/}\mathbf{n}_{/\!/} + \mathrm{P}_\perp \mathbf{n}_\perp + \mathrm{P}_{\mathrm{N}}\mathbf{n}_{\mathrm{N}} \ , \quad \boldsymbol{s}_t = s_{/\!/}\mathbf{n}_{/\!/} + s_\perp \mathbf{n}_\perp + s_{\mathrm{N}}\mathbf{n}_{\mathrm{N}} \ , \tag{33}$$

where the orthonormal basis is defined from the e^- beam direction and the top momentum direction:

$$\mathbf{n}_{/\!/} \equiv \frac{\boldsymbol{p}_e}{|\boldsymbol{p}_e|} \ , \quad \mathbf{n}_{\mathrm{N}} \equiv \frac{\boldsymbol{p}_e \times \boldsymbol{p}_t}{|\boldsymbol{p}_e \times \boldsymbol{p}_t|} \ , \quad \mathbf{n}_\perp \equiv \mathbf{n}_{\mathrm{N}} \times \mathbf{n}_{/\!/} \ . \tag{34}$$

Then the polarization of t is given by

$$(\mathrm{P}_{\mathrm{SM}})_{/\!/} = C_{/\!/}^0 + \mathrm{Re}\left(C_{/\!/}^1 \frac{F}{G}\right)\beta\cos\theta_{te} \ , \tag{35}$$

$$(\mathrm{P}_{\mathrm{SM}})_\perp = \mathrm{Re}\left(C_\perp \frac{F}{G}\right)\beta\sin\theta_{te} \ , \tag{36}$$

$$(\mathrm{P}_{\mathrm{SM}})_{\mathrm{N}} = \mathrm{Im}\left(C_{\mathrm{N}} \frac{F}{G}\right)\beta\sin\theta_{te} \tag{37}$$

for the contributions from the SM interactions[†], and

$$\delta\mathrm{P}_{/\!/} = 0 \ , \tag{38}$$

$$\delta\mathrm{P}_\perp = \left[\mathrm{Im}\left(B_\perp^g d_{tg}\frac{D}{G}\right) + \mathrm{Im}\left(B_\perp^\gamma d_{t\gamma}\frac{F}{G}\right) + \mathrm{Im}\left(B_\perp^Z d_{tZ}\frac{F}{G}\right)\right]\beta\sin\theta_{te} \ , \tag{39}$$

$$\delta\mathrm{P}_{\mathrm{N}} = \left[\mathrm{Re}\left(B_{\mathrm{N}}^g d_{tg}\frac{D}{G}\right) + \mathrm{Re}\left(B_{\mathrm{N}}^\gamma d_{t\gamma}\frac{F}{G}\right) + \mathrm{Re}\left(B_{\mathrm{N}}^Z d_{tZ}\frac{F}{G}\right)\right]\beta\sin\theta_{te} \tag{40}$$

[†] These results were derived in [30–32].

for the contributions from the anomalous interactions. The coefficients $C_{/\!/}^0$ etc. are defined below.

There is also a term bilinear in $\boldsymbol{s}_t$ and $\bar{\boldsymbol{s}}_t$, which represents the correlation of t and $\bar{t}$ spins:

$$(\boldsymbol{s}_t)_i(\bar{\boldsymbol{s}}_t)_j \mathbf{Q}_{ij} = (\boldsymbol{s}_t)_i(\bar{\boldsymbol{s}}_t)_j \left(\mathbf{Q}_{ij\,\mathrm{SM}} + \delta\mathbf{Q}_{ij} \right) \ , \tag{41}$$

where

$$(\boldsymbol{s}_t)_i(\bar{\boldsymbol{s}}_t)_j \mathbf{Q}_{ij\,\mathrm{SM}} = s_{/\!/}\bar{s}_{/\!/} + (s_{/\!/}\bar{s}_\perp + s_\perp\bar{s}_{/\!/})\,\mathrm{Re}\left(C_\mathrm{N}\frac{F}{G} \right) \beta \sin\theta_{te}$$

$$+ (s_{/\!/}\bar{s}_\mathrm{N} + s_\mathrm{N}\bar{s}_{/\!/})\,\mathrm{Im}\left(C_\perp\frac{F}{G} \right) \beta \sin\theta_{te} \ , \tag{42}$$

and

$$(\boldsymbol{s}_t)_i(\bar{\boldsymbol{s}}_t)_j\,\delta\mathbf{Q}_{ij} =$$

$$(s_{/\!/}\bar{s}_\perp - s_\perp\bar{s}_{/\!/})\left[\mathrm{Im}\left(B_\mathrm{N}^g d_{tg}\frac{D}{G} \right) + \mathrm{Im}\left(B_\mathrm{N}^\gamma d_{t\gamma}\frac{F}{G} \right) + \mathrm{Im}\left(B_\mathrm{N}^Z d_{tZ}\frac{F}{G} \right) \right] \beta \sin\theta_{te}$$

$$+ (s_{/\!/}\bar{s}_\mathrm{N} - s_\mathrm{N}\bar{s}_{/\!/})\left[\mathrm{Re}\left(B_\perp^g d_{tg}\frac{D}{G} \right) + \mathrm{Re}\left(B_\perp^\gamma d_{t\gamma}\frac{F}{G} \right) + \mathrm{Re}\left(B_\perp^Z d_{tZ}\frac{F}{G} \right) \right] \beta \sin\theta_{te} \ . \tag{43}$$

The coefficients C_i's and B_i^X's included in $\mathbf{P}_\mathrm{SM}$, $\delta\mathbf{P}$, $\mathbf{Q}_{ij\,\mathrm{SM}}$, $\delta\mathbf{Q}_{ij}$ are defined as follows. For the SM contributions,[‡]

$$C_{/\!/}^0(\chi) = -\frac{a_2 + \chi a_1}{a_1 + \chi a_2} \ , \qquad C_{/\!/}^1(\chi) = 2C_{/\!/}^0 C_\mathrm{N} + C_\perp = 2(1-\chi^2)\frac{a_2 a_3 - a_1 a_4}{(a_1 + \chi a_2)^2} \ ,$$

$$C_\perp(\chi) = -\frac{a_4 + \chi a_3}{a_1 + \chi a_2} \ , \qquad C_\mathrm{N}(\chi) = \frac{a_3 + \chi a_4}{a_1 + \chi a_2} = C_\mathrm{FB} \ . \tag{44}$$

The coefficients for the CP-odd contributions are given by

$$B_\perp^\gamma(\chi)\,d_{t\gamma} + B_\perp^Z(\chi)\,d_{tZ} = \frac{a_5 + \chi a_6}{a_1 + \chi a_2} \ ,$$

$$B_\mathrm{N}^\gamma(\chi)\,d_{t\gamma} + B_\mathrm{N}^Z(\chi)\,d_{tZ} = \frac{a_6 + \chi a_5}{a_1 + \chi a_2} \ , \tag{45}$$

[‡] Our notations are similar to those of [31, 32]. There are two differences: (i) our a_3 and a_4 are factor two smaller than theirs; (ii) our C_N is defined in opposite sign to theirs.

and

$$B^g_\perp(\chi) = -1 \ ,$$

$$B^\gamma_\perp(\chi) = \frac{1}{a_1 + \chi a_2} \left\{ \left([v^e v^t]^* v^{e\gamma} + [a^e v^t]^* a^{e\gamma} \right) + \chi \left([v^e v^t]^* a^{e\gamma} + [a^e v^t]^* v^{e\gamma} \right) \right\}$$

$$= \frac{1}{a_1 + \chi a_2} \left([v^e v^t]^* v^{e\gamma} + \chi [a^e v^t]^* v^{e\gamma} \right) \ ,$$

$$B^Z_\perp(\chi) = \frac{1}{a_1 + \chi a_2} \left\{ \left([v^e v^t]^* v^{eZ} + [a^e v^t]^* a^{eZ} \right) + \chi \left([v^e v^t]^* a^{eZ} + [a^e v^t]^* v^{eZ} \right) \right\} d(s) \ ,$$

$$B^g_{\mathrm{N}}(\chi) = C^0_{/\!/}(\chi) \ , \tag{46}$$

$$B^\gamma_{\mathrm{N}}(\chi) = \frac{1}{a_1 + \chi a_2} \left\{ \chi \left([v^e v^t]^* v^{e\gamma} + [a^e v^t]^* a^{e\gamma} \right) + \left([v^e v^t]^* a^{e\gamma} + [a^e v^t]^* v^{e\gamma} \right) \right\}$$

$$= \frac{1}{a_1 + \chi a_2} \left(\chi [v^e v^t]^* v^{e\gamma} + [a^e v^t]^* v^{e\gamma} \right) \ ,$$

$$B^Z_{\mathrm{N}}(\chi) = \frac{1}{a_1 + \chi a_2} \left\{ \chi \left([v^e v^t]^* v^{eZ} + [a^e v^t]^* a^{eZ} \right) + \left([v^e v^t]^* a^{eZ} + [a^e v^t]^* v^{eZ} \right) \right\} d(s) \ .$$

Symbols $a_{1\sim6}$ denote combinations of the electroweak parameters:

$$a_1 = \left| [v^e v^t] \right|^2 + \left| [a^e v^t] \right|^2 \ , \qquad\qquad a_2 = 2 \operatorname{Re} \left([v^e v^t]^* [a^e v^t] \right) \ , \tag{47}$$

$$a_3 = [v^e v^t]^* [a^e a^t] + [a^e v^t]^* [v^e a^t] \ , \qquad\qquad a_4 = [v^e v^t]^* [v^e a^t] + [a^e v^t]^* [a^e a^t] \ ,$$

and

$$a_5 = [v^e v^t]^* [v^e d^t] + [a^e v^t]^* [a^e d^t]$$
$$= [v^e v^t]^* v^{e\gamma} d_{t\gamma} + [v^e v^t]^* v^{eZ} d(s) \, d_{tZ} + [a^e v^t]^* a^{eZ} d(s) \, d_{tZ} \ ,$$

$$a_6 = [v^e v^t]^* [a^e d^t] + [a^e v^t]^* [v^e d^t] \tag{48}$$
$$= [v^e v^t]^* a^{eZ} d(s) \, d_{tZ} + [a^e v^t]^* v^{e\gamma} d_{t\gamma} + [a^e v^t]^* v^{eZ} d(s) \, d_{tZ} \ .$$

Symbols $[v^e a^t]$ etc. are defined in the Appendix, eq. (69), and $d(s)$ is the ratio of the Z propagator to the γ propagator [eq. (70)].

We comment here why there is no $\mathbf{n}_{/\!/}$ component in $\delta \mathbf{P}$ [eq. (38)] or why there are only a few components in $\delta \mathbf{Q}_{ij}$ [eq. (43)]. $\delta \mathbf{P}$ and $\delta \mathbf{Q}_{ij}$ originate from interferences of the leading SM amplitude M_0 and the amplitude proportional to the anomalous couplings δM. The SM amplitude M_0 is in a linear combination of spin $S_{/\!/} = \pm 1$ states $(c_+ | \uparrow\uparrow \rangle + c_- | \downarrow\downarrow \rangle)$, whereas the CP-reversed amplitude δM is in spin $S_{/\!/} = 0$ state $(| \uparrow\downarrow \rangle - | \downarrow\downarrow \rangle)$; see Sec. 2. In order to produce a non-zero interference between the two amplitudes, either one of the spins of t and $\bar{t}$ must be flipped. This is possible only by sandwitching the spin operator $\hat{S}^{(i)}_\perp$ or $\hat{S}^{(i)}_{\mathrm{N}}$ ($i = t$ or $\bar{t}$).

We can understand from symmetry considerations the combinations of the electroweak couplings and the Green functions in each term of the production cross section $\mathrm{d}\sigma(\boldsymbol{s}_t, \bar{\boldsymbol{s}}_t)/\mathrm{d}^3 \boldsymbol{p}_t$.
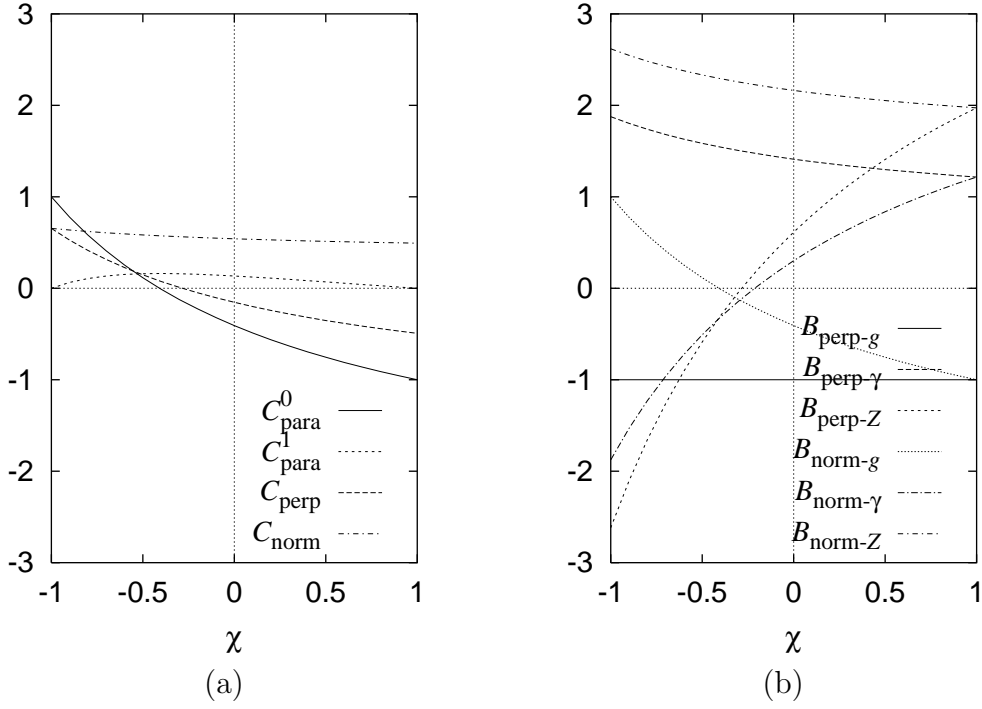
Figure 2: The electroweak coefficients C_i's and B_i^X's (for $\mathbf{P}$, $\bar{\mathbf{P}}$ and $\mathbf{Q}_{ij}$) vs. the initial $e^{\pm}$ polarization parameter χ. In the figures, $C_{\mathrm{para}} = C_{/\!/}$, $C_{\mathrm{perp}} = C_{\perp}$, $C_{\mathrm{norm}} = C_{\mathrm{N}}$, etc. (a) The coefficients for the SM contributions. (b) The coefficients for the contributions from the anomalous couplings.

This provides a non-trivial cross check of the formulas presented in this section; the argument is presented in [43].

5 Numerical Analyses of $\delta\mathbf{P}$ and $\delta\mathbf{Q}_{ij}$

In this section we study numerically the polarization vectors and the spin correlation tensor derived in the previous section. We use the input parameters: $m_{\mathrm{PS}}(\mu_f) = 175$ GeV, $\mu_f = 3$ GeV, $\mu = 20$ GeV, $m_Z = 91.19$ GeV, $\alpha_s(m_Z) = 0.118$, and $\sin^2\theta_W = 0.2312$.

First we examine the coefficients C_i's and B_i^X's, which represent combinations of electroweak couplings. They are given as a function of χ; cf. eq. (30). Fig. 2(a) shows the coefficients for the SM contributions $\mathbf{P}_{\mathrm{SM}}$ and $\mathbf{Q}_{ij\,\mathrm{SM}}$. Except for $C_{/\!/}^1$, typical sizes of the coefficients are order one. Fig. 2(b) shows the coefficients for the CP-violating contributions $\delta\mathbf{P}$ and $\delta\mathbf{Q}_{ij}$. Typical sizes of all these coefficients are order one. We see that their dependences on χ are different.

Next we examine the S-wave and P-wave Green functions. In Figs. 3(a) and (b) are shown the Green functions at $E = -2$ GeV and $E = +2$ GeV, respectively. They depend on both the energy E and the top momentum p_t. The momentum distribution of top quark $d\sigma/\mathrm{d}^3\boldsymbol{p}_t \propto p_t^2|G(E, p_t)|^2$ has a peak ($p_t = p_{\mathrm{peak}}$) at a given c.m. energy [26], see Figs. 4 and 5. Then we may plot the ratios $\beta F/G$ and $\beta D/G$, included in $\delta\mathbf{P}$ and $\delta\mathbf{Q}_{ij}$, as a function of the energy E alone by choosing the top momentum to be the peak momentum p_{peak}. These are
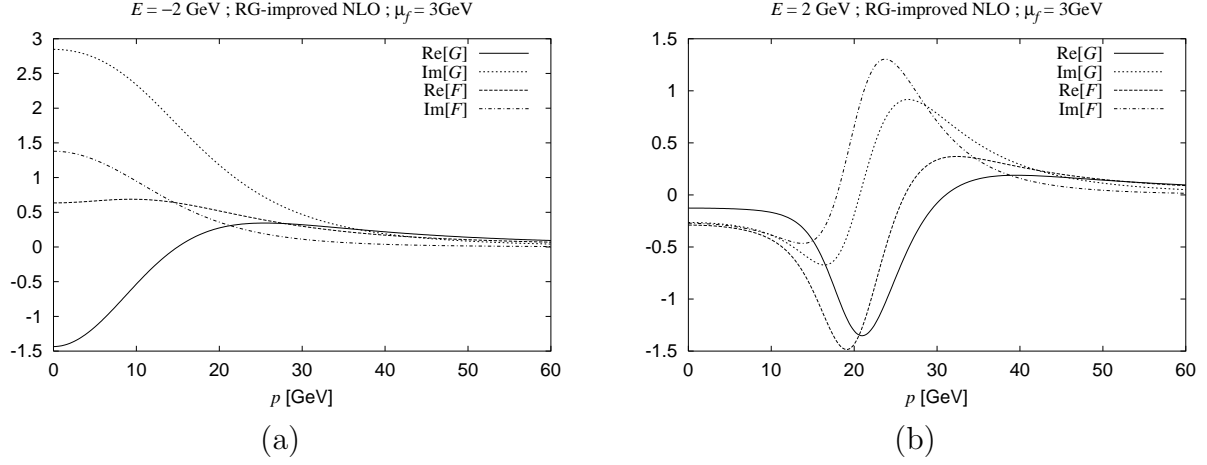
Figure 3: The S-wave and P-wave Green functions vs. the top quark momentum p at (a) $E = -2$ GeV, (b) $E = +2$ GeV.
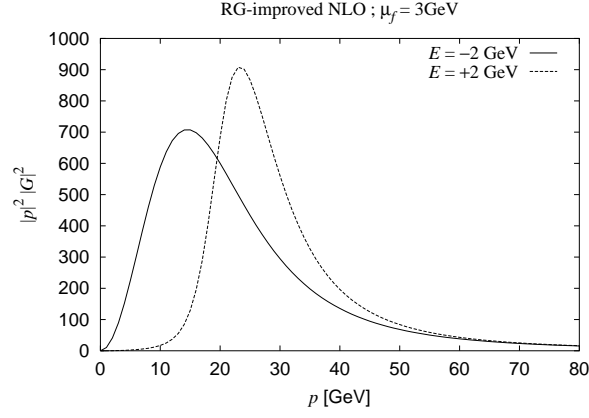

Figure 4: $p^2|G(E,p)|^2$ vs. the top quark momentum p at fixed c.m. energies. These are proportional to the leading-order momentum distributions of top quark.
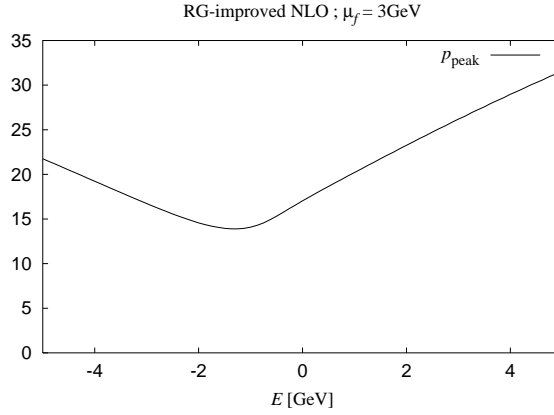

Figure 5: The peak momentum p_{peak} of the momentum distribution $\mathrm{d}\sigma/\mathrm{d}p \propto |\boldsymbol{p}|^2|G|^2$ vs. the c.m. energy measured from the twice of the potential-subtracted mass, $E = \sqrt{s} - 2m_{\text{PS}}(\mu_f)$. It represents the typical momentum of top quark as a function of E.
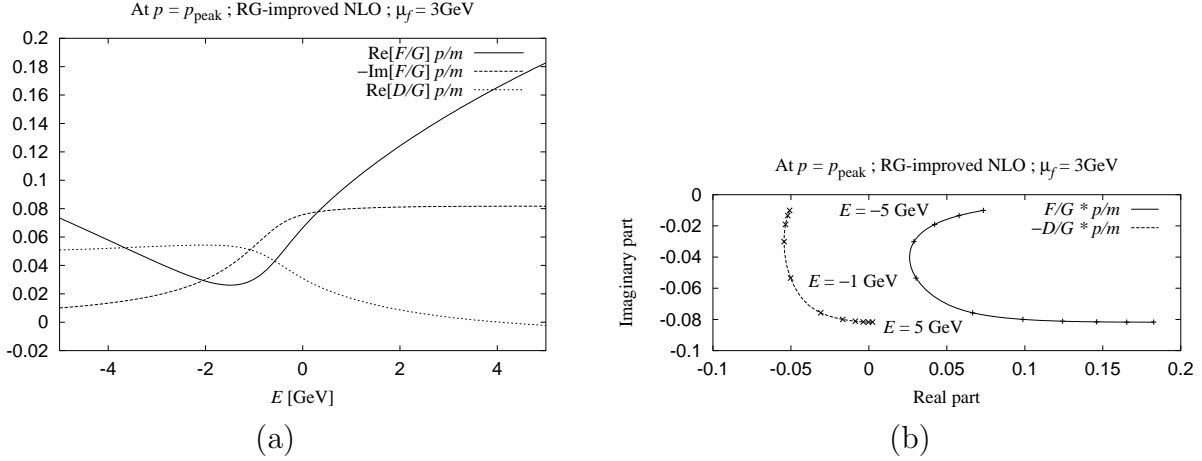
Figure 6: The ratios of the Green functions times the "velocity" of top quark evaluated at the peak momentum p_{peak} of the momentum distribution $d\sigma/dp$; see Fig. 5. (a) These are given as a function of E. (b) These are plotted on a complex plane as E is varied.

shown in Figs. 6. We see that the size of $|\beta F/G|$ is 5–20% while the size of $|\beta D/G|$ is 5–10%. Clearly their energy dependences are different. Also it can be seen that the strong phases are quite sizable.

One may understand these behaviors of the Green functions semi-quantitatively using analytic formulas. The relation

$$p_{\text{peak}} \simeq \left| \sqrt{m_t \left(E + 1\,\text{GeV} + i\Gamma_t \right)} \right| \tag{49}$$

agrees qualitatively with Fig. 5, in particular at $E > 0$.[§] Here, $1\,\text{GeV} \simeq 2m_t - M_{1S} =$ "binding energy". For a stable quark pair with the Coulomb potential, G and F can be obtained analytically for on-shell kinematics [44]:

$$\lim_{\substack{\Gamma_t \to 0 \\ E \to p_t^2/m_t}} \left(E - \frac{\boldsymbol{p_t}^2}{m_t} + i\Gamma_t \right) G(E, p_t) \bigg|_{V=V_{\text{C}}} = \exp\left(\frac{\pi p_{\text{B}}}{2p_t} \right) \Gamma\left(1 + i\frac{p_{\text{B}}}{p_t} \right) , \tag{50}$$

$$\lim_{\substack{\Gamma_t \to 0 \\ E \to p_t^2/m_t}} \left(E - \frac{\boldsymbol{p_t}^2}{m_t} + i\Gamma_t \right) F(E, p_t) \bigg|_{V=V_{\text{C}}} = \left(1 - i\frac{p_{\text{B}}}{p_t} \right) \exp\left(\frac{\pi p_{\text{B}}}{2p_t} \right) \Gamma\left(1 + i\frac{p_{\text{B}}}{p_t} \right) , \tag{51}$$

where $p_{\text{B}} \equiv C_F \alpha_s m_t/2 \simeq 20\,\text{GeV}$. Thus, we may find a sensible approximation formula

$$\frac{F}{G}\bigg|_{p=p_{\text{peak}}} \simeq 1 - i\frac{p_{\text{B}}}{\sqrt{m_t \left(E + 1\,\text{GeV} + i\Gamma_t \right)}} . \tag{52}$$

This agrees qualitatively well with Figs. 6. It follows that $D/G \to 0$ and $F/G \to 1$ when $|E + i\Gamma_t| \gg \alpha_s^2 m_t$.

Combining the analyses of the electroweak coefficients and the Green functions, we find that the typical sizes of the CP-odd quantities $\delta\mathbf{P}$ and $\delta\mathbf{Q}_{ij}$ are 5–20% times the couplings

___

[§] For $V \to 0$, $p_{\text{peak}} = \left| \sqrt{m_t \left(E + i\Gamma_t \right)} \right|$ holds exactly.

16

$(d_{t\gamma}, d_{tZ}, d_{tg})$ in the threshold region. Using the different dependences on the $e^{\pm}$ polarizations and on the c.m. energy, we will be able to disentangle the effects of the three anomalous couplings in the $t\bar{t}$ threshold region. A more comprehensive numerical study of the coefficients and the Green functions is presented in [43].

6   Observables and Sensitivity Estimates

So far we have considered the CP-odd quantities related to the spins of t and $\bar{t}$. These quantities are, however, not directly measurable observables in experiments. In this section we focus on $\delta\mathbf{P}$ and consider how to extract it. Then we give rough estimates of sensitivities to the CP-violating couplings $d_{t\gamma}$, d_{tZ}, d_{tg} expected at future e^+e^- colliders.

The top quark polarization vector can be extracted most efficiently using the angular distribution of charged leptons from the decay of top quarks. The charged lepton angular distribution in the $t\bar{t}$ threshold region, in the leading order, is given by

$$\frac{\mathrm{d}\sigma(e^+e^- \to t\bar{t} \to b\ell^+\nu\bar{b}W^-)}{\mathrm{d}^3\boldsymbol{p}_t \mathrm{d}\Omega_\ell} \simeq \frac{\mathrm{d}\sigma}{\mathrm{d}^3\boldsymbol{p}_t} \times \frac{1}{\Gamma_t} \frac{\mathrm{d}\Gamma_{t\to b\ell^+\nu}(\mathbf{P})}{\mathrm{d}\Omega_\ell} \ . \tag{53}$$

The left-hand-side shows that this is the differential cross section where the three-momentum of parent top quark and the direction of charged lepton are fixed, while all other variables are integrated over. The right-hand-side shows that it is given as a product of the $t\bar{t}$ production cross section eq. (29) and the decay angular distribution from free polarized top quarks. The top polarization vector is given by eq. (31). The lepton angular distribution in the top rest frame is given by eq. (5). It coincides with the angular distribution in the laboratory frame in the leading order, since top quarks are almost at rest in the threshold region. Hence, the expectation value of the lepton three-momentum projected onto an arbitrary chosen direction $\mathbf{n}$ is proportional to the top quark polarization vector in the same approximation [31]:

$$\langle\langle \mathbf{n} \cdot \boldsymbol{p}_\ell \rangle\rangle \simeq \frac{1 + 2r + 3r^2}{12(1 + 2r)} m_t \times \mathbf{n} \cdot \mathbf{P} \ , \tag{54}$$

where $r = m_W^2/m_t^2$, and $\langle\langle \cdots \rangle\rangle$ denotes an average taken for a fixed top three-momentum $\boldsymbol{p}_t$.

Taking a CP-odd combination, the contributions of the anomalous interactions can be extracted as

$$\langle\langle \mathbf{n} \cdot (\boldsymbol{p}_\ell + \bar{\boldsymbol{p}}_\ell) \rangle\rangle \simeq \frac{1 + 2r + 3r^2}{6(1 + 2r)} m_t \times \mathbf{n} \cdot \delta\mathbf{P} \ . \tag{55}$$

By choosing $\mathbf{n} = \mathbf{n}_\perp$ and $\mathbf{n}_N$, we can extract the components eqs. (39) and (40) of $\delta\mathbf{P}$. The above formula remains valid even if we include the full $\mathcal{O}(\alpha_s)$ corrections (in particular the final-state interactions) in the SM parts of eqs. (53) [32] and (54) [31], since the pure SM contributions drop in the CP-odd combination. Alternatively, we may consider a slightly different observable

$$\langle\langle \mathbf{n} \cdot (\mathbf{n}_\ell + \bar{\mathbf{n}}_\ell) \rangle\rangle \simeq \frac{2}{3} \mathbf{n} \cdot \delta\mathbf{P} \ , \tag{56}$$

where $\mathbf{n}_\ell/\bar{\mathbf{n}}_\ell$ denote the directions of $\ell^{\pm}$. This observable would be useful if the $\ell^{\pm}$ directions can be measured more accurately than their three-momenta, such as in the case of $\tau^{\pm}$.

In experiments the lepton-plus-4-jet mode can be used to reconstruct the lepton momentum and the top quark three-momentum simultaneously [29]. In order to detect a signal of CP-violation, it is not necessary to reconstruct the top quark three-momentum with a high accuracy. One should define the top quark momentum merely as the sum of all the visible momenta in a top-jet cluster, so no stringent cuts are required to reduce missing momentum. The only important point is that any experimental cut should be imposed in a CP symmetric way. Later when we measure accurately the values of the couplings $d_{t\gamma}$, d_{tZ}, d_{tg}, we would need to reconstruct the top quark three-momentum to a reasonable accuracy.

In order to extract $\delta\mathbf{Q}_{ij}$ we need to measure spin correlations of t and $\bar{t}$. Instead of eq. (53) we should consider a double differential decay distribution of t and $\bar{t}$, which can be obtained using the formula of [45]. We may think of observables such as $\langle(\boldsymbol{p}_t-\bar{\boldsymbol{p}}_t)\cdot(\boldsymbol{p}_\ell\times\bar{\boldsymbol{p}}_\ell)\rangle$ for CP-odd observables sensitive to $\delta\mathbf{Q}_{ij}$. Here, we do not discuss extraction of $\delta\mathbf{Q}_{ij}$ any further and leave the subject to our future work.

Let us make rough estimates of sensitivities to the CP-violating couplings $d_{t\gamma}$, d_{tZ}, d_{tg} expected in future experiments. Eq. (56) shows that a statistical reconstruction of the top quark polarization using lepton directions is quite efficient. The top quark polarization vector projected to a certain direction $\mathrm{P} = \langle\boldsymbol{s}_t\cdot\mathbf{n}\rangle$ is given by

$$\mathrm{P} \simeq \frac{N_\uparrow - N_\downarrow}{N_\uparrow + N_\downarrow} ,\tag{57}$$

where $N_\uparrow$ ($N_\downarrow$) denotes the number of top quarks with spin in the direction $\mathbf{n}$ ($-\mathbf{n}$). Hence, the statistical error of P may be estimated as $\delta^{(\text{stat})}\mathrm{P} \sim 1/\sqrt{N_{\text{eff}}}$, where N_{eff} stands for the number of events used for the analysis. Assuming an integrated luminosity $\int\mathcal{L} = 50\,\text{fb}^{-1}$ and a detection efficiency $\epsilon = 0.6$,

$$\begin{aligned} N_{\text{eff}} &= \sigma_{t\bar{t}} \times \textstyle\int\mathcal{L} \times (2B_\ell B_h) \times \epsilon \\ &\simeq 0.5\,\text{pb} \times 50\,\text{fb}^{-1} \times \left(2\cdot\frac{2}{9}\cdot\frac{2}{3}\right) \times 0.6 = 4\times10^3\,\text{events}, \end{aligned}\tag{58}$$

which means $1/\sqrt{N_{\text{eff}}} \simeq 1.5\times10^{-2}$. The leptonic (hadronic) branching fraction B_ℓ (B_h) of $W^\pm$ into $e^\pm$ and $\mu^\pm$ (hadrons) is given by 2/9 (2/3).

Using the relations

$$\delta\mathrm{P}_\perp = \mathrm{Im}\left(B_\perp^g d_{tg}\frac{D}{G}\right)\beta\sin\theta_{te} , \quad \delta\mathrm{P}_\mathrm{N} = \mathrm{Re}\left(B_\mathrm{N}^g d_{tg}\frac{D}{G}\right)\beta\sin\theta_{te} ,\tag{59}$$

the statistical error of d_{tg} is estimated to be

$$\begin{aligned} \delta^{(\text{stat})}d_{tg} &\sim \frac{1}{|B_i^g D/G|\beta} \times \frac{\int_{-1}^{1}\mathrm{d}(\cos\theta_{te})\,1}{\int_{-1}^{1}\mathrm{d}(\cos\theta_{te})\,\sin\theta_{te}} \times \frac{1}{\sqrt{N_{\text{eff}}}} \\ &\simeq \frac{1}{0.1} \times \frac{4}{\pi} \times 1.5\times10^{-2} \\ &\simeq 0.2 \sim \mathcal{O}(10\%) . \end{aligned}\tag{60}$$

Note that we have similar sensitivities to both the real part and imaginary part of d_{tg} independently using the two components of the top quark polarization vector. The above value translates to a sensitivity to the chromo-EDM of top quark at

$$\delta^{(\text{stat})} \left(\frac{g_s}{m_t} d_{tg} \right) \sim 10^{-17} g_s \, \text{cm} \ . \tag{61}$$

Since all the electroweak coefficients ($C_\perp$, B_{N}, etc.) are of similar sizes, and so are the ratios of the Green functions ($\text{Im} \, (F/G)$, etc.), sensitivities to the EDM and Z-EDM are estimated to be at the same order:

$$\delta^{(\text{stat})} \left(\frac{e}{m_t} d_{t\gamma} \right) \sim 10^{-17} e \, \text{cm} \ , \quad \delta^{(\text{stat})} \left(\frac{g_Z}{m_t} d_{tZ} \right) \sim 10^{-17} g_Z \, \text{cm} \ . \tag{62}$$

A Monte Carlo simulation study is also in progress incorporating realistic experimental conditions expected at a future e^+e^- collider [46]. They show that high detection efficiency is possible with simple event selection criteria and b-tagging. Up to now, only the lepton energy asymmetry $\langle E_{\ell^+} - E_{\ell^-} \rangle$ for the dilepton-plus-2-jet events was studied [47]. The 1σ statistical error corresponding to $100 \, \text{fb}^{-1}$ was obtained as

$$\delta^{(\text{stat})} \left[\langle E_{\ell^+} - E_{\ell^-} \rangle \right] = 0.65 \, \text{GeV} \ . \tag{63}$$

They studied the bounds on the anomalous couplings setting the input values to be $d_{t\gamma} = d_{tZ} = d_{tg} = 0$. Based on our calculations, they obtained $|\text{Re}[e^{i\phi_\gamma} d_{t\gamma}]| < 1.5$, $|\text{Re}[e^{i\phi_Z} d_{tZ}]| < 1.0$, $|\text{Re}[e^{i\phi_g} d_{tg}]| < 3.9$ at 95% confidence-level (statistical errors only), where $e^{i\phi_X}$'s are the relevant strong phases. In fact, the lepton energy asymmetry is not a good observable for extracting $\delta\mathbf{P}$ in the threshold region. It is suppressed by $\beta \sim 10\%$ compared to the CP-odd combination of the lepton three-memontum, eq. (55). Moreover the branching fraction for the lepton-plus-4-jet mode is larger than that for the dilepton-plus-2-jet mode. Thus, we expect that the sensitivities to the anomalous EDMs will be better by a factor 10 or more if we use the lepton three-momentum or the lepton direction. This is consistent with the naive estimates we made above.

7 Summary and Conclusions

In this paper we studied how to probe the anomalous CP-violating couplings of top quark with γ, Z and g in the $t\bar{t}$ threshold region at future e^+e^- colliders. The anomalous couplings contribute to the difference of the t and $\bar{t}$ polarization vectors, $\delta\mathbf{P} = (\mathbf{P} - \bar{\mathbf{P}})/2$, as well as to the spin correlation tensor $\delta\mathbf{Q}_{ij}$. We studied dependences of these CP-odd quantities on the $e^\pm$ beam polarizations, c.m. energy, and top quark momentum. We find that the typical sizes of $\delta\mathbf{P}$ and $\delta\mathbf{Q}_{ij}$ are 5–20% times the couplings $(d_{t\gamma}, d_{tZ}, d_{tg})$ in the threshold region. Experimentally we can measure $\delta\mathbf{P}$ efficiently using the expectation value of the CP-odd combination of the $\ell^\pm$ momenta, $\boldsymbol{p}_\ell + \bar{\boldsymbol{p}}_\ell$, or of the $\ell^\pm$ directions, $\mathbf{n}_\ell + \bar{\mathbf{n}}_\ell$. We have similar sensitivities to both the real part and imaginary part of $d_{t\gamma}$, d_{tZ}, d_{tg} independently using the two components of the top quark polarization vector $\delta\text{P}_\perp$ and $\delta\text{P}_{\text{N}}$. Taking advantage of different dependences of $\delta\mathbf{P}$

on the $e^\pm$ polarizations and on the c.m. energy, we will be able to disentangle the effects of the three anomalous couplings $d_{t\gamma}$, d_{tZ}, d_{tg} in the $t\bar{t}$ threshold region. We made rough estimates of sensitivities to the anomalous couplings expected at future e^+e^- colliders, considering as a simplest example extraction of $\delta\mathbf{P}$ from the $\ell^\pm$ distributions. For an integrated luminosity of 50 fb^{-1}, we estimated

$$\delta^{(\text{stat})}d_{t\gamma},\ \delta^{(\text{stat})}d_{tZ},\ \delta^{(\text{stat})}d_{tg} \sim \mathcal{O}(10\%) \tag{64}$$

when only one of the couplings is turned on at a time.¶ The above values translate to sensitivities to the top quark EDM, Z-EDM and chromo-EDM:

$$\delta^{(\text{stat})}\left(\frac{e}{m_t}d_{t\gamma}\right) \sim 10^{-17}e\,\text{cm}\ ,\quad \delta^{(\text{stat})}\left(\frac{g_Z}{m_t}d_{tZ}\right) \sim 10^{-17}g_Z\,\text{cm}\ ,$$
$$\delta^{(\text{stat})}\left(\frac{g_s}{m_t}d_{tg}\right) \sim 10^{-17}g_s\,\text{cm}\ . \tag{65}$$

The sensitivities to the top quark EDM and Z-EDM are comparable to those attainable in the open-top region at e^+e^- colliders [17]. The sensitivity to d_{tg} is worse than that expected at a hadron collider [3, 4, 10, 13–16] but exceeds the sensitivity in the open-top region at e^+e^- colliders [21]. We note that there is an advantage of the $t\bar{t}$ threshold region. The clean environment of an e^+e^- collider enables accurate determination of the value of the top-gluon anomalous coupling d_{tg} if its value happens to be larger than $\mathcal{O}(10\%)$. On the other hand, at hadron colliders it would be difficult to measure the value of the coupling with a similar accuracy even if a CP-violating effect is detected. Regarding energy upgrading scenario of a future linear e^+e^- collider, it is possible that the machine operates first in the $t\bar{t}$ threshold region for a significant amount of time, while measuring the top quark mass precisely, etc., before the beam energies will be increased to the open-top region. Therefore it would be desirable that measurements of the anomalous couplings can be performed concurrently with other unique measurements near threshold, with sensitivities comparable to those in the open-top region. Unfortunately the sensitivities to the CP-violating couplings achievable in the $t\bar{t}$ threshold region are one to three orders of magnitude larger than the predicted sizes of top quark EDMs in the models reviewed in Sec. 1. Using the results of this work, a Monte Carlo study incorporating realistic experimental conditions expected at a future e^+e^- linear collider is underway [46].

Acknowledgements

¶ We would be able to improve the sensitivities by using other observables: $\delta\mathbf{P}$ can be extracted also from distributions of charm quarks from $W^\pm$ instead of $\ell^\pm$; $\delta\mathbf{Q}_{ij}$ can be extracted using correlations of $\ell^\pm$, b, c distributions.

Appendix: Conventions and Notations

In $e^+e^- \to t\bar{t}$, both γ and Z are exchanged in s-channel. Their effects can be combined in terms of effective couplings. We denote the SM vertices for electron and top quark by

$$\Lambda_{X\mu} = g_X \left(v^{eX} \gamma_\mu - a^{eX} \gamma_\mu \gamma_5 \right) , \qquad \Gamma_X^\mu = g_X \left(v^{tX} \gamma^\mu - a^{tX} \gamma^\mu \gamma_5 \right) \qquad (X = \gamma, Z) , \qquad (66)$$

where

$$g_\gamma = e = g \sin\theta_W , \quad v^{f\gamma} = Q_f , \quad a^{f\gamma} = 0 ,$$
$$g_z = \frac{g}{\cos\theta_W} , \quad v^{fZ} = \frac{1}{2} T_{3L} - Q_f \sin^2\theta_W , \quad a^{fZ} = \frac{1}{2} T_{3L} . \qquad (67)$$

The amplitude for $e^+e^- \to t\bar{t}$ at tree level can be written as

$$\sum_{X=\gamma,Z} \frac{1}{s - m_X^2} \left(\bar{v}(\bar{p}_e) \Lambda_{X\mu} u(p_e) \right) \left(\bar{u}(p_t) \Gamma_X^\mu v(\bar{p}_t) \right)$$
$$= \frac{e^2}{s} \Big[\quad [v^e v^t] \left(\bar{v}(\bar{p}_e) \gamma_\mu u(p_e) \right) \left(\bar{u}(p_t) \gamma^\mu v(\bar{p}_t) \right)$$
$$- [v^e a^t] \left(\bar{v}(\bar{p}_e) \gamma_\mu u(p_e) \right) \left(\bar{u}(p_t) \gamma^\mu \gamma_5 v(\bar{p}_t) \right)$$
$$- [a^e v^t] \left(\bar{v}(\bar{p}_e) \gamma_\mu \gamma_5 u(p_e) \right) \left(\bar{u}(p_t) \gamma^\mu v(\bar{p}_t) \right)$$
$$+ [a^e a^t] \left(\bar{v}(\bar{p}_e) \gamma_\mu \gamma_5 u(p_e) \right) \left(\bar{u}(p_t) \gamma^\mu \gamma_5 v(\bar{p}_t) \right) \Big] , \qquad (68)$$

where

$$[v^e v^t] = v^{e\gamma} v^{t\gamma} + d(s) \, v^{eZ} v^{tZ} ,$$
$$[v^e a^t] = v^{e\gamma} a^{t\gamma} + d(s) \, v^{eZ} a^{tZ} = d(s) \, v^{eZ} a^{tZ} ,$$
$$[a^e v^t] = a^{e\gamma} v^{t\gamma} + d(s) \, a^{eZ} v^{tZ} = d(s) \, a^{eZ} v^{tZ} , \qquad (69)$$
$$[a^e a^t] = a^{e\gamma} a^{t\gamma} + d(s) \, a^{eZ} a^{tZ} = d(s) \, a^{eZ} a^{tZ}$$

represent energy-dependent "couplings". Extensions to the anomalous vertices should be obvious. $d(s)$ is the ratio of the Z propagator to the γ propagator

$$d(s) \equiv \frac{g_z^2}{e^2} \frac{s}{s - m_Z^2 + i m_Z \Gamma_Z} \qquad (70)$$

with

$$\frac{g_z^2}{e^2} = \frac{\left(\frac{g}{\cos\theta_W} \right)^2}{(g \sin\theta_W)^2} = \frac{1}{\cos^2\theta_W \sin^2\theta_W} = 5.625 . \qquad (71)$$

The width Γ_Z of Z introduces an absorptive part. At $\sqrt{s} = 2 \times 175 \, \text{GeV}$, its relative magnitude is $s/(s - m_Z^2 + i m_Z \Gamma_Z) = 1.073 - 0.002\,i$. Thus, in the threshold region, the Coulomb binding effects overwhelm the effect of Γ_Z. Also in the open-top region, it is known that the QCD correction is larger than the effect of Γ_Z, as far as the normal component of the polarization of top quark P_N is concerned.

References

[1] I. B. Khriplovich, Yad. Fiz. **44**, 1019 (1986) [Sov. J. Nucl. Phys. **44**, 659 (1986)]; Phys. Lett. **B173**, 193 (1986);
A. Czarnecki and B. Krause, Acta Phys. Polon. **B28**, 829 (1997); Phys. Rev. Lett. **78**, 4339 (1997).

[2] W. Bernreuther, T. Schröder and T. N. Pham, Phys. Lett. **B279**, 389 (1992);
A. Soni and R. M. Xu, Phys. Rev. Lett. **69**, 33 (1992).

[3] C. R. Schmidt and M. E. Peskin, Phys. Rev. Lett. **69**, 410 (1992).

[4] W. Bernreuther and A. Brandenburg, Phys. Lett. **B314**, 104 (1993); Phys. Rev. D **49**, 4481 (1994);
W. Bernreuther, A. Brandenburg and M. Flesch, hep-ph/9812387.

[5] D. Chang, W.-Y. Keung, I. Philips, Nucl. Phys. **B408**, 286 (1993); (E) *ibid.* **B429**, 255 (1994); Phys. Rev. D **48**, 3225 (1993);
A. Pilaftsis and M. Nowakowski, Int. J. Mod. Phys. **A9**, 1097 (1994); (E) *ibid.* **A9**, 5849 (1994).

[6] W. Bernreuther and P. Overmann, Z. Phys. C **61**, 599 (1994); Z. Phys. C **72**, 461 (1996).

[7] M. S. Baek, S. Y. Choi and C. S. Kim, Phys. Rev. D **56**, 6835 (1997).

[8] W. Bernreuther, A. Brandenburg and P. Overmann, hep-ph/9602273.

[9] A. Bartl, E. Christova, T. Gajdosik and W. Majerotto, Nucl. Phys. **B507**, 35 (1997); (E) *ibid.* **B531**, 653 (1998).

[10] C. R. Schmidt, Phys. Lett. **B293**, 111 (1992).

[11] B. Grządkowski and W.-Y. Keung, Phys. Lett. **B316**, 137 (1993); Phys. Lett. **B319**, 526 (1993);
B. Grządkowski, Phys. Lett. **B305**, 384 (1993);
A. Bartl, E. Christova and W. Majerotto, Nucl. Phys. **B460**, 235 (1996); (E) *ibid.* **B465**, 365 (1996);
A. Bartl, E. Christova, T. Gajdosik and W. Majerotto, Phys. Rev. D **58**, 074007 (1998); Phys. Rev. D **59**, 077503 (1999);
E. Christova, Int. J. Mod. Phys. **A14**, 1 (1999);
W. Hollik, J. I. Illana, S. Rigolin, C. Schappacher, and D. Stöckinger, Nucl. Phys. **B551**, 3 (1999).

[12] P. Haberl, O. Nachtmann and A. Wilch, Phys. Rev. D **53**, 4875 (1996);
K. Cheung and D. Silverman, Phys. Rev. D **55**, 2724 (1997);
J. L. Hewett, T. Takeuchi, and S. Thomas, hep-ph/9603391;
J. L. Hewett, Int. J. Mod. Phys. **A13**, 2389 (1998).

[13] D. Atwood, A. Aeppli and A. Soni, Phys. Rev. Lett. **69**, 2754 (1992).

[14] T. G. Rizzo, Phys. Rev. D **53**, 6218 (1996).

[15] A. Brandenburg and J. P. Ma, Phys. Lett. **B298**, 211 (1993);
K. Cheung, Phys. Rev. D **53**, 3604 (1996); Phys. Rev. D **55**, 4430 (1997);
S. Y. Choi, C. S. Kim and Jake Lee, Phys. Lett. B **415**, 67 (1997).

[16] G. L. Kane, G. A. Ladinsky and C.-P. Yuan, Phys. Rev. D **45**, 124 (1992);
C.-P. Yuan, Mod. Phys. Lett. **A10**, 627 (1995);
S. Bar-Shalom and G. Eilam, hep-ph/9810234.

[17] R. Frey, hep-ph/9606201;
R. Frey *et al.*, hep-ph/9704243.

[18] D. Atwood and A. Soni, Phys. Rev. D **45**, 2405 (1992).

[19] W. Bernreuther, O. Nachtmann, P. Overmann and T. Schröder, Nucl. Phys. **388**, 53
(1992); (E) *ibid.* **406**, 516 (1993);
W. Bernreuther and P. Overmann, Z. Phys. C **61**, 599 (1994); Z. Phys. C **72**, 461 (1996);
G. A. Ladinsky and C.-P. Yuan, Phys. Rev. D **49**, 4415 (1994);
P. Poulose and S. D. Rindani, Phys. Lett. **B349**, 379 (1995); Phys. Rev. D **54**, 4326
(1996); Phys. Lett. **B383**, 212 (1996);
B. Grządkowski and Z. Hioki, Nucl. Phys. **B484**, 17 (1997); Phys. Lett. **B391**, 172 (1997);
hep-ph/9805318;
L. Brzezínski, B. Grządkowski, and Z. Hioki, Int. J. Mod. Phys. **A14**, 126 (1999);
M. S. Baek, S. Y. Choi and C. S. Kim, Phys. Rev. D **56**, 6835 (1997);
S. Lietti and H. Murayama, hep-ph/0001304.

[20] F. Cuypers and S. D. Rindani, Phys. Lett. **B343**, 333 (1995).

[21] T. G. Rizzo, hep-ph/9610373;
S. D. Rindani and M. M. Tung, Phys. Lett. **B424**, 125 (1998); Eur. Phys. J. **C11**, 485
(1999).

[22] H. Anlauf, W. Bernreuther, and A. Brandenburg, Phys. Rev. D **52**, 3803 (1995); (E)
ibid. **53**, 1725 (1996);
S. Y. Choi and K. Hagiwara, Phys. Lett. **B359**, 369 (1995);
P. Poulose and S. D. Rindani, Phys. Rev. D **57**, 5444 (1998); Phys. Lett. **B452**, 347
(1999).

[23] V.S. Fadin and V.A. Khoze, JETP Lett. **46**, 525 (1987); Sov. J. Nucl. Phys. **48**, 309
(1988).

[24] M. Strassler and M. Peskin, Phys. Rev. **D43**, 1500 (1991).

[25] R. Guth and J. Kühn, Nucl. Phys. **B368**, 38 (1992).

[26] Y. Sumino, K. Fujii, K. Hagiwara, H. Murayama and C.-K. Ng, Phys. Rev. **D47**, 56 (1993);
M. Jeżabek, J.H. Kühn and T. Teubner, Z. Phys. **C56**, 653 (1992).

[27] H. Murayama and Y. Sumino, Phys. Rev. **D47**, 82 (1993).

[28] K. Melnikov and O. Yakovlev, Phys. Lett. **B324**, 217 (1994).

[29] K. Fujii, T. Matsui and Y. Sumino, Phys. Rev. **D50**, 4341 (1994).

[30] R. Harlander, M. Jeżabek, J.H. Kühn and T. Teubner, Phys. Lett. **B346**, 137 (1995).

[31] R. Harlander, M. Jeżabek, J. Kühn and M. Peter, Z. Phys. **C73**, 477 (1997).

[32] M. Peter and Y. Sumino, Phys. Rev. **D57**, 6912 (1998).

[33] A. Hoang and T. Teubner, Phys. Rev. **D58**, 114023 (1998);
K. Melnikov and A. Yelkhovsky, Nucl. Phys. **B528**, 59 (1998);
O. Yakovlev, Phys. Lett. **B457**, 170 (1999);
A. Penin and A. Pivovarov, Nucl. Phys. **B549**, 217 (1999); hep-ph/9904278;
M. Beneke, A. Signer and V. Smirnov, Phys. Lett. **B454**, 137 (1999);
A. Hoang and T. Teubner, Phys. Rev. **D60**, 114027 (1999).

[34] T. Nagano, A. Ota and Y. Sumino, Phys. Rev. **D60**, 114014 (1999).

[35] J. Kühn and T. Teubner, Eur. Phys. J. **C9**, 221 (1999).

[36] J. Kühn, Acta Phys. Pol. **B12**, 347 (1981).

[37] J. Kühn and K. Streng, Nucl. Phys. **B198**, 71 (1982);
M. Jeżabek, J. Kühn, Nucl. Phys. **B320**, 20 (1989).

[38] B. Grządkowski and Z. Hioki, hep-ph/9911505.

[39] M. Beneke, Phys. Lett. **B434**, 115 (1998).

[40] F. Feinberg, Phys. Rev. Lett. **39**, 316 (1977); Phys. Rev. **D17**, 2659 (1978).

[41] R. Karplus and A. Klein, Phys. Rev. **87**, (1952) 848.

[42] J. Kühn and P. Zerwas, Phys. Rep. **167**, 321 (1988).

[43] T. Nagano, PhD thesis, Tohoku University, 2000 (in preparation).

[44] V. Fadin, V. Khoze and M. Kotsky, Z. Phys. **C64**, 45 (1994).

[45] Y. Tsai, Phys. Rev. **D4**, 2821 (1971);
S. Kawasaki, T. Shirafuji and S. Tsai, Prog. Theor. Phys. **49**, 1656 (1973).

[46] K. Ikematsu, K. Fujii, Z. Hioki, T. Nagano, S. Rindani, Y. Sumino and T. Takahashi, in preparation.

[47] K. Ikematsu, to appear in the Proceedings of *the Second ACFA Workshop on Physics/Detector at the Linear Collider*, Seoul, Korea, Nov. 1999.